J. Amer. Soc. Hort. Sci. 147(3):161–173. 2022. https://doi.org/10.21273/JASHS05157-21

Complex Plant Process Trait Evaluation Through Decomposition of Higher-order Interaction: A Case Study in Acclimation Responses of Cold-climate Hybrid Grapevine Through Bilinear and Multiway Methods

John E. Stenger
Department of Agriculture and Biosystems Engineering, North Dakota State University Department 7620, P.O. Box 6050, Fargo, ND 58108-6050

Harlene M. Hatterman-Valenti
Department of Plant Sciences, North Dakota State University Department 7520, P.O. Box 6050, Fargo, ND 58108-6050

Additional index words. environment, interspecific, singular value decomposition, temperature, Tucker decomposition, *Vitis riparia*

Abstract. **Traditionally, the structure of higher-order data in genotype-by-environment interaction requires simplification to use bilinear reduction models. Flexible multiway reduction models have been claimed to be more informative, as they allow exploration of individual trends and account for the covariance among data modes. In complex latent traits, such as acclimation response of grapevine (*Vitis* sp.), these methods may offer increased insight into plant adaptive processes. In a growth chamber study, data from seven phenotypic traits at 11 photoperiodic times in the presence of two temperatures of 30 accessions were analyzed. The four-way interaction among these data modes was isolated and further examined through bilinear singular value decomposition (SVD) and multiway Tucker decomposition models. A similar set of three latent process traits were identified regardless of model used. The Tucker decomposition model led to more concise clustering of wild-type accessions, was more interpretable, as trends could be evaluated separately, and had less indication of overfitting; therefore, the multiway method was preferred over the standard SVD bilinear method in the investigation of high-order interaction in acclimation response. This methodology may offer insight into other complex traits, such as phenolic development, drought tolerance, and horizontal disease resistance to improve breeding efforts as other individual mechanisms used by the organism are separated, quantified, and compared rather than the culmination of events as an end-product.**

The development of cold-hardy grapevine (*Vitis* sp.) cultivars in the 1990s created a growing industry in the upper Midwest and northern Great Plains regions of the United States. However, the inadequacy in combining overwintering ability with high fruit quality has limited financial stability of continental viticulture and its associated wine industry. Climate conditions in non-coastal regions are relatively unpredictable when compared with more traditional coastal U.S. and Mediterranean production areas. For this reason, large temperature fluctuations are likely to impact vine progress in its transition from active growth to a dormant resting state. To stabilize production in these northern regions of the United States through cultivar development, methods are needed to comparatively analyze cultivar adaptive capabilities under differing temperatures during the fall, particularly during short-duration deviations in plant alterations due to dynamic temperature swings.

Acclimation to winter conditions is an example of a biological process and can be categorized as a latent construct. Many environmental cues influence a vine, causing a cascade of physiological and physical alterations leading to a state of tolerance to winter stresses with the ability to survive these stresses and reinitiate growth on the return of favorable conditions. Grapevine responses to either photoperiod or temperature have been identified and extensively studied (Burke et al., 1976; Fennell and Hoover, 1991; Fennell et al., 2005, 2015; Garris et al., 2009; Schnabel and Wample, 1987; Smita et al., 2021; Wake and Fennell, 2000). Gaining a better understanding of comparative acclimation processes among accessions through time under dynamic environmental conditions may result in improved breeder selection for local adaptation. Allusions to the potential for such environmentally adaptive traits have been made in prior study; however, more foundational investigations have yet to be reported (Garris et al., 2009). In addition, the complexity of grapevine acclimation is not unique. Traits such as stress tolerance, horizontal disease resistance, and flavor and aroma development, as well as metabolic and transcriptomic expression are areas of importance in numerous crops and are difficult to quantify due to their complexity, latency, and time-dependent nature.

Received for publication 26 Nov. 2022. Accepted for publication 25 Mar. 2022. Published online 31 May 2022.
This work was supported by the U.S. Department of Agriculture, Agricultural Marketing Service, North Dakota Department of Agriculture Specialty Crop Block Grant (NDDA 17-135), North Dakota Grape, Wine and Fruit Promotion Grant (FAR0028705), and the North Dakota State University Graduate School Doctoral Dissertation Fellowship. We thank Collin Auwarter for his help in conducting this study.
H.M.H.-V. is the corresponding author: E-mail: h.hatterman.valenti@ndsu.edu.

Tools are needed to adequately separate distinct processes that lead to similar quantifiable outcomes such that each may be evaluated individually. Such traits, resulting in similar phenotypic outcomes, are typically confounded in traditional evaluations, as only the product of their conjoined effects is quantified. The quantification of processes is inherently difficult and involves many inputs leading to varied outcomes that may or may not be directly quantifiable. These inputs and outcomes are likely to have multiple levels of correlation with one another depending on the conditions with varying degrees of covariation over time. When applied to a natural setting, these influencing factors are not applied at a constant rate nor do all occur at predictable timings, causing difficulties in analysis and interpretation of results. To facilitate selection, the complex process of grapevine acclimation has been analyzed as a single cause leading to a single effect (Garris et al., 2009; Fennell and Hoover, 1991; Fennell et al., 2005; Wake and Fennell, 2000). This methodology has been used in other multivariate areas, such as metabolomics, alongside multivariate methods (Goodacre et al., 2007). Although the treatment of latent process traits as univariate causes and effects has allowed progress, only a portion of the genetic potential is being exploited because the intercorrelation of predictor variables, the intercorrelation of outcomes, and cross relationships are ignored as the quantitative trait is forced into a qualitative solution. A more recent evaluation used transcriptomic approaches to assess differential responses in paired accessions of adapted riparian grapevine (*Vitis riparia*) and a French-American interspecific hybrid cultivar Seyval (Fennell et al., 2015). Additional assessments have been made in expression patterns of an individual riparian grapevine accession as plants transition from a long-day condition that fostered paradormancy to a short-day condition that fostered endodormancy (Smita et al., 2021). Although such studies are important in assessing the underlying genetic mechanism responsible for differences in metabolic responses to decreasing photoperiod, such studies are limited in accession number and environmental scope. In the current study, under the assumption that more information could be obtained by observing much of the dataset, bilinear and multiway data reduction methods were used to reduce a multivariate dataset of reactionary responses of a diverse set of interspecific hybrid grapevines as affected by temperature and decreasing photoperiod through time.

Traditionally, to evaluate the environmentally dependent relative performance of cultivars through trait stability analysis, interactions are dissected using bilinear factor-analytic models (Flores et al., 1998; Piepho, 1999). One such reduction model that may be applied to any matrix of arbitrary dimension is SVD. Although SVD can be used to reduce multiway data arrays through the concatenation of multiple modes to form combination-mode matrices, this practice ignores the covariance among concatenated modes (Cong et al., 2015; Kroonenberg, 2008; Mørup, 2011). In addition, through multiway decomposition, each mode is individually reduced into components allowing easier interpretation of individual data mode trends.

Higher-order decompositions are extensions of bilinear methods to facilitate multimode datasets and have been applied to the decomposition of three-way data to deconstruct genotype-by-environment interactions in latent composite traits (Chapman et al., 1997; Van Eeuwijk and Kroonenberg, 1998). Tensor-based multiway deconstruction methods also have been applied to timeseries data. Nesaragi et al. (2021) used multiway decomposition to investigate time-based interactions among data in medical records to successfully and reliably predict sepsis. In the current study, multiway investigation of latent trait genotype-by-environment interaction was extended to four modes with the addition of time as the Tucker4 decomposition model to extend the evaluation of latent composite traits to latent composite processes and will be compared with traditional evaluation of bilinear decomposition using combination-mode matrices.

Many of the vine traits that affect vineyard production, reliability, and quality are best described as processes. Understanding of how end-products are reached, rather than merely their final value, will be paramount to moving from breeding for high phenotypic performance to breeding for consistent performance as the underlying mechanisms resulting in similar outcomes are separated and critically evaluated. In this study, a flexible higher-order multiplicative model was compared with a more traditional bilinear SVD model. Emphasis was placed on their relative abilities to model a four-way interaction effect to separate riparian grapevine and nonriparian grapevine acclimation types, ability to interpret their resulting trends, and their ability to define a stable subspace in which comparisons could be made.

Materials and Methods

Plant material. Thirty accessions were propagated for investigation. Several S0 progenitor grapevines, non-inbred interspecific grapevines resulting from crosses of non-inbred parents, were used to derive several S1 progeny as the result of S0 self-pollination. These S1 progeny vines were derived from 'Valiant' (64 and 73), 'MN 1131' (900, 903, and 906), 'St. Croix' (909, 911, 913, and 914), 'ES 8-2-24' (917, 920, and 924), and 'ES 8-2-43' (936, 937, 938, 939, and 940). Although it was intended to have five progenies from each family, due to rooting or vernalization failure, some accessions were eliminated through the course of the study. 'Valiant' and 'St. Croix' are of fox grapevine (*Vitis labrusca*), riparian grapevine, and common grapevine (*Vitis vinifera*) descent; whereas 'MN 1131', 'ES 8-2-24', and 'ES 8-2-43' are largely of riparian and common grapevine descent having less fox grapevine parentage [Hemstad, 2015; Hemstad and Luby, 2000; Swenson, 1982; U.S. Department of Agriculture, Agricultural Research Service (USDA-ARS), 2022]. 'Valiant' is a first-generation descendent of a riparian grapevine from eastern Montana, whereas 'MN 1131', 'ES 8-2-24', and 'ES 8-2-43' are first-generation descendants of the riparian grapevine 89, a wild vine collected in Minnesota and parent used extensively in northern grapevine breeding noted not to acclimate early in Minnesota; however, having early leaf senescence (USDA-ARS, 2022). 'MN 1131', 'Marquette', and 'Frontenac' were included as regional industry standard checks.

Several native riparian grapevine accessions were used to emulate trait diversity of vines exhibiting fitness for survival in important production regions of North Dakota, including locations near the Red River of the North and portions of northwestern North Dakota and northeastern Montana. Vine fitness was assessed as those collected vines having large-caliper trunks and showing significant old-wood above any prospective snowline indicating several years of growth without significant winter kill, or an accession having substantial use in cold-climate grapevine breeding. These accessions were included to compare interspecific hybrid responses to the wild-type responses of vines proven successful in the northern Plains region of the United States.

Accession 1002 was collected near the Sheyenne River near Kindred, ND. Accessions 1001 and 1003 were collected near the Red River of the North near Abercrombie and Fargo, ND, respectively. Accession 1004 was received under the designation Rip 821 and originated near Burlington, ND. Accession SD 62-8-160 (PI 588269) is documented as having early maturity and leaf senescence and originating by the Missouri River near Culbertson, MT (USDA-ARS, 2022). SD 62-8-160 has its origin consistent with the parentage of 'Valiant', whereas the geographic origins of all other tested riparian grapevines were intermediate between that of the parentage of 'Valiant' and other tested accessions and related families derived from sources in Minnesota (riparian grapevines 89 and Carver).

A collection of california grapevine (*Vitis californica*) was added as an outgroup (956, 958, 961, 962, and 965), as several attempts to evaluate genetic relationships within the grapevine genus have placed the california grapevine as an outgroup of the North American species (Pèros et al., 2011; Trŏndle et al., 2010; Wan et al., 2013; Zecca et al., 2012). In addition, the species provided examples of a North American native species from a region having a Mediterranean climate more typical of the Eurasian common grapevine species. The seed of the california grapevine accessions was obtained commercially (Sheffield Seed Co., Locke, NY). Because the seed was obtained from a commercial source, the likelihood of potential genetic contamination from introduced species, such as common grapevine or riparian grapevine, is unknown, as well as the degree of inbreeding within the obtained seed.

Growing conditions. Regardless of the material source, individual mother plants were used to propagate test plants. Propagules were rooted using green shoot tip cuttings in 100% perlite while being treated with 0.1% indole-3-butyric acid powder (Hormodin 1; OHP, Midland, PA). While rooting, all cuttings from the same mother plant were placed within a single 8.89-cm plastic pot. Pots were placed in a plastic film chamber and received constant bottom heat using a heating cable and were periodically misted using a household humidifier. Well-rooted plantlets were selected and planted in cone-shaped containers [6.35 cm diameter, 25.4 cm height (D40H Deepots; Stuewe and Sons, Tangent, OR)] with soilless medium (Sunshine Mix #1; Sun Gro Horticulture, Agawam, MA). Of rooted vines, the most homogeneous plantlets within each accession were retained for observation. Before the initiation of each growth chamber run, plants were vernalized for 6 weeks in a cooler at 3 °C to induce budbreak. On removal from cold treatment, plants were pruned to four-node spurs as near to soil level as possible and root pruned to a length of ~10.2 cm to prevent root binding and were replanted in the same container as they were vernalized. Plants were then placed in a walk-in growth chamber [≈500 $\mu mol \cdot m^{-2} \cdot s^{-1}$ (model no. WE-95; Percival Scientific, Perry, IA)] for the duration of the experiment. Each plant was restricted to a single shoot arising nearest to soil level and was trained to a bamboo stake. Tying to promote upward growth occurred weekly and as needed based on individual vine vigor. Vines were irrigated daily to capacity and were given weekly applications of 20N–4.4P–16.6K water-soluble fertilizer following data collection at a rate of 400 $g \cdot L^{-1}$ N to support growth. Vines grew for 3 weeks at a photoperiod of 16 h daylight and a temperature of 27 °C before any reduction in photoperiod or temperature treatment initiation.

Experimental design. Plants were evaluated at 10 and 27 °C at separate times in the same chamber. Within each replication-by-temperature run of the growth chamber, four sample vines of each accession were evaluated. Each test vine was randomly assigned to one of four blocks within each experimental run-by-temperature combination consistent with a randomized complete block design combined across experimental run-by-temperature combinations.

Dormancy was evaluated similar to previous studies with modifications (Fennell and Hoover, 1991; Fennell et al., 2005; Garris et al., 2009; Wake and Fennell, 2000). For each of the four run-by-temperature combinations, test plants were subjected to decreasing photoperiod starting with 15 h daylight followed by 9 h darkness. Light hours were reduced weekly by 0.5 h for 10 weeks to an ending photoperiod of 10 h daylight and 14 h darkness. Acclimation measures were quantified at the end of each week for each 0.5 h decrease in photoperiod resulting in 11 photoperiodic data collection periods.

For data collection, plants were removed from the growth chamber where they were evaluated for shoot length (centimeters), number of nodes, number of mature nodes, number of lateral shoots, tip growth cessation (0–5 scale), and periderm development (centimeters and number of nodes encompassed). Shoot length was measured from the base of the actively growing shoot to its tip. Number of nodes was counted as the number of buds along the actively growing shoot. Mature nodes were counted at the first signs of mature woody tissue development on bud scales. Presence of lateral shoots was determined at the time of its first unfurled leaf. Tip abscission was visibly assessed on a scale of 0 (full active growth) to 5 (complete tip abscission). Intermediary responses were assessed as decreasing levels of tip elongation (1–2) and increasing levels of meristem browning and necrosis (3–4). Mature periderm was measured as both a length and as buds encompassed. Mature periderm length was measured as the distance from the base of the actively growing shoot to the extent of shoot showing mature woody periderm. Mature periderm development as nodes encompassed was measured as the count of nodes that were encompassed by this measured length of stem having mature periderm. Mature periderm as nodes encompassed was included as an easier implemented alternative to length measurements. In addition, it was thought that counting of nodes encompassed by stem periderm development would be less biased by natural vine stature, thus both measurements of periderm development were included. Last, node maturation and periderm development measured as nodes encompassed were functionally different, as many accessions demonstrate periderm development encompassing nodes before any indication of woody development of bud scales at such nodes or have buds mature before periderm development. Following data collection, vines were arbitrarily replaced within their designated replications to ensure overall homogeneous conditions per vine. Within the chamber, vines were placed in contiguous rows, each spaced one pot width apart, thus each vine was given a 6.4 × 19.1-cm area in which to grow.

Statistical analysis. Within each trait, least squares means were estimated for mode combinations using the MIXED procedure of SAS statistical software (version 9.4; SAS Institute, Cary, NC). Estimated means were used to construct the four-mode dataset (run-by-accession, measures, photoperiods, and temperatures). The modes relating to runs of the experiment and accessions were concatenated to create a mode termed "sample"

to retain each experimental replication as a replication of accessions for further comparison between models. To isolate the four-way interaction, data were fiber centered for each mode and measures were scaled to a common variance due to their differing units using the nprocess function of the N-way Toolbox for MATLAB (version R2015a; MathWorks, Natick, MA) (Andersson and Bro, 2000). The quadruple centering of the data effectively removed all main effects and lower-level interactions leaving only the effects of the four-way interaction (Kroonenberg, 2008). As the comparison among accessions in relative reaction trends between temperatures was the focus of this study, lower-level interactions were not reintroduced to the dataset and only the four-way interaction was interpreted.

When SVD was used, the modes of measures, photoperiods, and temperatures were concatenated, resulting in a wide combination-mode matrix of dimension 60 × 154. SVD was conducted using the svds procedure of MATLAB statistical software as follows:

$$X = U\Sigma V' + E$$

where X was the n-x-m matrix containing the original data. U was the n-x-k matrix containing n sample scores relating to the k reduced axes, Σ was the diagonal k-x-k matrix containing singular values of the k reduced dimensions relating U to V, and V was the m-x-k matrix containing m variable loadings of the k reduced dimensions. E was the n-x-m matrix containing residuals of the model created from the reduction in dimensionality. The number of retained axes was determined as the best compromise between explained variance and model complexity by the visible evaluation of a scree plot.

A Tucker4 decomposition, an extension of the Tucker3 model, was applied to the four-mode data array [samples (A) × measures (B) × photoperiods (C) × temperatures (D)] of dimension 60 × 7 × 11 × 2 using the tucker function of the N-way Toolbox for MATLAB. The Tucker4 model takes the following form:

$$X_a = AG_a[D \otimes (C \otimes B)]' + E_a$$

where X_a was the n-x-m-x-p-x-q multiway array of centered and scaled interaction effects, G_a was a multiway array of size a-x-b-x-c-x-d containing the singular values of the associations between the reduced number of retained axes of mode matrices A (n-x-a), B (m-x-b), C (p-x-c), and D (q-x-d). The Kronecker product of two matrices was represented by ⊗, and E_a was the n-x-m-x-p-x-q multiway array containing residuals of the model due to the reduction in dimensionality of the four respective data modes. The number of axes retained for each mode was determined by visible inspection as the compromise between model complexity and retained variance of all mode axis combinations.

Following each data reduction, the sample scores were interpreted using analysis of variance (ANOVA). This method for interpretation of factors from decomposition was accomplished before and has been termed principal component analysis (PCA)-ANOVA (Légère and Samson, 1999; Luciano and Næs, 2009; Nomme and Harrison, 1991; Teh et al., 2010; Tomic et al., 2016). ANOVA was completed using the MIXED procedure of SAS statistical software as a randomized complete block design with two runs of the experiment treated as random replications of the 30 accessions, which were considered fixed effects. Mean values for S1 families, species, combined S1s, checks, and all nonriparian grapevine accessions were estimated. Single df contrasts were used to compare estimated mean values of accessions and groups of interest with the mean value of tested riparian grapevines to draw conclusions on their similarity.

To evaluate the grouping of riparian grapevines, data were also clustered using the DISTANCE and CLUSTER procedures of SAS statistical software using Euclidean distance among accession mean values with Ward's minimum variance method of linkage. Last, to compare the relative accuracy and consistency of the models, the sum of squared deviations from observed values as well as from the full model solutions, those containing all observed samples, were estimated for excluded samples in each of 10,000 iterations of resampling with replacement (50 train to 10 test) and compared using estimated 95% confidence intervals. Deviations from observed four-way interaction effects were used as an indicator of model fit, whereas deviations from full model solutions were used as an indicator of subspace stability.

Results

The centering of all data modes combined with two temperatures resulted in the mode's reduction to a single vector, as each value was half the distance from the mean. This occurred before the reduction of the data, as data were centered, and resulted in a functional reduction of the data to a three-mode dataset of differences between temperatures (temperature/2). For this reason, axes relating to temperature are not further discussed in either model.

Singular value decomposition

The optimum number of axes was three, on visible inspection of a scree plot of explained variance (Table 1). These components combined to recover 74.4% of the variation in the centered and scaled data, accounting for 34.1%, 29.5%, and 10.8% of the variance, respectively. Tabulated variable weights were visibly evaluated to determine that Axis 1 related to relative differences in tip abscission progression through photoperiodic time from 15.0 to 10.5 h of daylight between the two temperatures (Table 2). Axis 2 related to the relative transition in relative amounts of active growth and tissue maturation between early and late season between temperatures. In addition, this axis contrasted tip abscission progress at 14.5 h with 11.0 h of daylight.

Table 1. Singular value decomposition singular values, eigenvalues, proportions, and cumulative proportions of the total variance resulting from the reduction of higher-order interaction effects of grapevine response to simulated fall conditions between differing temperatures through photoperiodic time.

Axis[z]	Singular value	Eigenvalue	Proportion (%)	Cumulative (%)
1	**9.81**	**96.2**	**34.1**	**34.1**
2	**9.12**	**83.1**	**29.5**	**63.6**
3	**5.52**	**30.5**	**10.8**	**74.4**
4	3.41	11.6	4.1	78.5
5	3.07	9.4	3.3	81.9
6	2.93	8.6	3.0	84.9
7	2.41	5.8	2.1	87.0
8	2.27	5.1	1.8	88.8
…[y]	…	…	…	…
Total (154)	67.92	282.0	1	1

[z]Bolded components were retained for further interpretation.
[y]Rows relating to axes 9–154 were omitted.

Table 2. Factor weights of seven predictor variables across photoperiodic time determined using singular value decomposition of higher-order interaction effects in grapevine response to simulated fall conditions under differing temperatures for the first three retained axes.

		Daylight (h)										
Axis	Trait[z]	15.0	14.5	14.0	13.5	13.0	12.5	12.0	11.5	11.0	10.5	10.0
1												
	L	0.32[y]	0.19	−0.01	−0.20	−0.18	−0.19	−0.25	−0.12	0.02	0.14	0.28
	N	0.69	0.55	0.30	0.07	−0.16	−0.30	−0.36	−0.31	−0.23	−0.17	−0.09
	MAT	0.06	0.26	0.33	0.35	0.50	0.34	0.32	−0.24	−0.52	−0.67	−0.72
	LAT	0.25	−0.14	−0.58	−0.63	−0.74	−0.37	−0.36	0.25	0.53	0.77	1.03
	TIP	−2.33	−2.16	−1.7	−1.45	−1.03	0.23	0.90	1.60	2.05	2.14	1.74
	PL	0.53	0.68	0.85	0.98	0.88	0.19	−0.20	−0.64	−0.98	−1.13	−1.15
	PN	0.48	0.63	0.81	0.88	0.73	0.10	−0.05	−0.54	−0.88	−1.07	−1.09
2												
	L	1.01	1.08	0.95	0.67	0.30	−0.32	−0.83	−0.87	−0.84	−0.67	−0.48
	N	1.41	1.43	1.26	0.99	0.24	−0.40	−0.91	−1.08	−1.16	−0.94	−0.76
	MAT	−1.03	−0.92	−0.90	−0.69	−0.07	0.23	0.82	0.59	0.65	0.62	0.68
	LAT	1.98	1.73	1.29	0.89	0.11	−0.51	−1.31	−1.22	−1.24	−0.92	−0.80
	TIP	−0.91	−1.11	−0.67	−0.28	−0.24	0.20	0.13	0.62	1.10	0.75	0.44
	PL	−1.39	−1.27	−1.15	−0.96	−0.32	0.41	1.12	1.14	0.93	0.79	0.69
	PN	−1.06	−0.94	−0.78	−0.54	−0.02	0.39	0.98	0.81	0.56	0.36	0.24
3												
	L	1.40	0.65	0.07	−0.88	−1.91	−2.18	−1.30	0.01	0.75	1.49	1.91
	N	1.14	0.41	−0.35	−0.90	−1.99	−2.15	−1.21	−0.01	0.78	1.97	2.31
	MAT	−1.60	−1.17	−0.24	0.49	2.00	2.12	1.31	−0.08	−0.75	−0.71	−1.37
	LAT	1.16	1.13	0.00	−1.33	−2.6	−3.12	−1.51	0.38	1.42	2.01	2.46
	TIP	0.11	1.21	1.29	1.88	1.38	0.85	0.36	0.84	−0.56	−3.04	−4.32
	PL	−1.21	−1.29	−0.66	0.06	0.91	1.84	1.08	−0.28	−0.35	−0.27	0.16
	PN	−0.99	−0.96	−0.11	0.67	2.21	2.64	1.28	−0.85	−1.30	−1.45	−1.14

[z]L = stem length (centimeters); N = number of nodes; MAT = number of mature nodes; LAT = number of lateral shoots; TIP = tip abscission progress visible rating (0–5), where 0 relates to full active growth and 5 relates to loss of meristem; PL = periderm development length (centimeters); and PN = number of nodes enveloped by periderm development.
[y]Increasing green and red hues indicate increasingly positive and negative associations between the axis with the trait measure at the photoperiodic time, respectively.

Axis 3 was associated with parabolic distortion of the Axis 2 through photoperiodic time across the two tested temperatures. The axis also contrasted tip abscission progress at 12.5 h with that at 10.0 h of daylight. When these axes were tested with ANOVA, using runs of the experiment as replications, accessions differed across all three retained axes (Axis 1, $P = 0.0076$; Axis 2, $P = 0.0211$; and Axis 3, $P = 0.0432$).

When means of accessions, populations, groups, and species were compared with the mean of tested riparian grapevines, significant deviations occurred along all three axes (Table 3). Riparian grapevines were positively associated with all three axes. Of the included check cultivars, Frontenac did not differ from the mean of tested riparian grapevines along any axis. Both 'MN 1131' and 'Marquette' deviated from the response of the tested native accessions along Axis 1, whereas 'Marquette' also deviated along Axis 2. Axis 1 tended to be most associated with the accessions 'Frontenac' and 917, and most negatively associated with 'MN 1131' and its progeny. Only accessions having large negative values differed in response from riparian grapevines.

Axis 2 tended to be positively associated with 'MN 1131', its progeny 900, and the mean of riparian grapevines. The axis was negatively associated with progeny of 'ES 8-2-43', except for 937. In addition, 73 and 'Marquette' also differed from the mean of riparian grapevines along the axis.

Axis 3 was predominately associated with riparian grapevines as well as 900, and negatively associated with several accessions arising from diverse families (64, 906, 911, 920, 937, and 940). Of the included checks, all three were found to have positive values and none were found to significantly depart from the values of the tested native accessions. Only two accessions, 'Frontenac' and 917, were similar to the mean of tested riparian grapevine accessions across all three retained axes.

Two distinct groups formed when the mean values of the 30 tested accessions were clustered using Euclidean distance with Ward's minimum variance method of linkage (Fig. 1). 'Marquette' and 'Frontenac' clustered together, whereas 'MN 1131' differed. The tested riparian grapevines were split among groups; however, representatives in either group tended to cluster together within subgroups. In the group associated with 'Marquette' and 'Frontenac'; riparian grapevines, SD 62-8-160, and 1002 grouped along with 'Frontenac', 917, and 73, whereas 'Marquette' was associated with four of the five progenies of ES 8-2-43, 920, and 911. Within the 'MN 1131' group, two subgroups pertaining to riparian grapevine and nonriparian grapevine classes existed. The three remaining riparian grapevines clustered together, whereas 'MN 1131' clustered tightly with its progeny, as well as the remaining accessions derived from other families.

Tucker decomposition

On evaluation of the explained variance, all combinations of components for all modes, it was determined that the best fit was found using the reduced dimensions of 3 × 2 × 2 × 1 for the original 60 × 7 × 11 × 2 dataset. This solution explained 72.0% of the

Table 3. Comparison of mean accession scores obtained through singular value decomposition and Tucker decomposition resulting from the reduction of higher-order interaction effects of grapevine response to simulated fall conditions between differing temperatures through photoperiodic time.

	Singular value decomposition						Tucker decomposition					
Accession	Axis 1		Axis 2		Axis 3		Axis 1		Axis 2		Axis 3	
64	−0.008		−0.034		−0.152	**	−0.005		−0.027		0.145	
73	0.139		−0.088	*	0.053		0.142		−0.084	*	−0.042	
900	−0.164	**[z]	0.195		0.102		−0.168	**	0.186		−0.086	
903	−0.164	**	0.039		0.055		−0.163	**	0.034		−0.030	
906	−0.097	*	0.064		−0.121	**	−0.099	*	0.064		0.116	
909	−0.133	**	−0.022		−0.057	*	−0.131	**	−0.019		0.027	
911	0.019		−0.023		−0.158	**	0.019		−0.023		0.157	
913	−0.050		0.079		−0.056	*	−0.051		0.072		0.047	
914	−0.127	*	0.026		−0.031		−0.130	*	0.020		0.035	
917	0.155		0.033		−0.047		0.153		0.038		0.042	
920	0.059		−0.046		−0.129	**	0.060		−0.040		0.139	
924	0.087		−0.061		−0.052	*	0.088		−0.055		0.043	
936	−0.024		−0.137	**	−0.055	*	−0.019		−0.135	**	0.045	
937	−0.136	**	0.045		−0.130	**	−0.138	**	0.044		0.126	
938	−0.004		−0.089	*	0.042		−0.002		−0.091	*	−0.047	
939	−0.079	*	−0.143	**	−0.017		−0.076		−0.145	**	0.037	
940	0.013		−0.090	*	−0.128	**	0.016		−0.089	*	0.129	
‘Frontenac’	0.157		−0.053		0.009		0.159		−0.045		−0.014	
‘MN 1131’	−0.192	**	0.101		0.018		−0.198	***	0.092		−0.020	
‘Marquette’	−0.106	*	−0.083	*	0.043		−0.106	*	−0.090	*	−0.048	
	Estimated family means											
‘Valiant’[y]	0.065		−0.061	*	−0.049	*	0.069		−0.055	*	0.052	
‘MN 1131’	−0.141	****	0.100		0.012		−0.143	****	0.095		0.000	
‘St. Croix’	−0.073	**	0.015		−0.076	***	−0.073	**	0.012		0.067	
‘ES 8-2-24’	0.100		−0.025	*	−0.076	**	0.100		−0.019	*	0.075	
‘ES 8-2-43’	−0.046	**	−0.083	***	−0.058	***	−0.044	*	−0.083	***	0.058	
	Estimated mean effect of important groups of accessions											
Checks	−0.047	*	−0.011		0.023		−0.048	*	−0.014	*	−0.027	
All S1s	−0.030	**	−0.015	**	−0.052	****	−0.03	**	−0.015	**	0.052	
Non-*V. rip*[x]	−0.015	*	−0.018	**	−0.020	**	−0.014	*	−0.019	**	0.021	
V. cali[x]	0.057		−0.034	**	0.063		0.058		−0.037	**	−0.054	
V. rip[x]	0.074	–	0.091	–	0.099	–	0.071	–	0.095	–	−0.106	–
P value[w]	0.0076		0.0211		0.0432		0.0072		0.0254		0.0976	

[z]*, **, ***, and **** signify that the value is significantly different from that of the mean of riparian grapevines within the associated component at alpha = 0.05, 0.01, 0.001, and 0.0001, respectively.
[y]Estimated mean of S1 progeny of the listed S0 parental vine.
[x]Non-*V. rip* = nonriparian grapevine, *V. cali* = california grapevine; *V. rip* = riparian grapevine.
[w]Probability of a greater *F* from analysis of variance of each axis using the respective model. Comparisons with riparian grapevines were only evaluated in axes where accessions were found to vary ($\alpha = 0.05$).

variation that existed in the original interaction data. The solution's core-array suggested that four relationships among the resulting components had the greatest influence on the dataset (Table 4).

Measures. Using the Tucker model, two axes were defined from the initial seven phenotypic traits measured (Table 5). Axis 1 largely contrasted measures of growth with tissue maturation. Stem length, number of nodes, and number of lateral shoots were positively associated with the axis, whereas the number of mature buds and measures of periderm development were negatively associated. The strongest positive association with the axis was with measures of periderm development, whereas the most negative association was with measures of number of lateral shoots. This axis was considered the relative progress of the transition from active growth (negative) to the maturation of tissues (positive).

Axis 2 was most strongly and positively associated with progress toward tip abscission. The axis was marginally, negatively associated with the number of nodes. Axis 2 was characterized as progress toward tip abscission and the cessation shoot tip growth.

Photoperiods. Two significant axes were found for photoperiodic time from the original 11 time points collected. Axis 1 was interpreted to be general progress through time with photoperiod 14.5 h of daylight being positively and 10.5 h of daylight being negatively associated with the axis with a gradual transition between these photoperiodic extremes. Axis 2 was interpreted as a parabolic distortion from the linear trend through time and was centered around 12.5 h of daylight.

Variable weights. When the full set of the reduced phenotypic axes was used to construct the variable effects associated

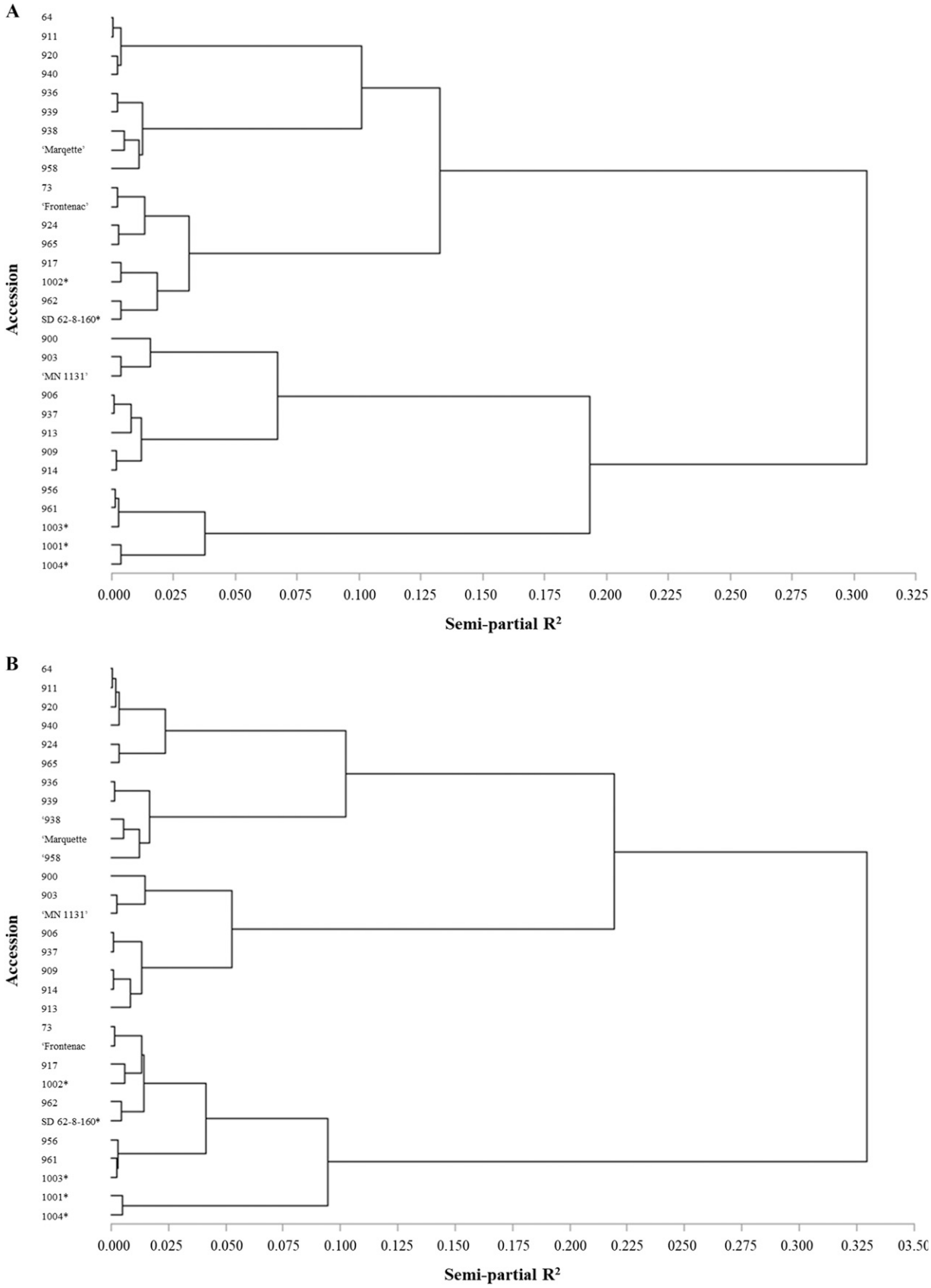

Fig. 1. Cluster of Euclidean distances between grapevine accession means from the decompositions of the four-way interaction effects of grapevine accessions grown under differing temperatures through photoperiodic time using (**A**) singular value decomposition and (**B**) Tucker decomposition using Ward's minimum variance method of linkage. Presence of * indicates riparian grapevine accessions.

Table 4. Tucker decomposition core-array of relationships between grapevine accession, predictor trait measures, and photoperiod axes resulting from the reduction of higher-order interaction effects of grapevine response to simulated fall conditions between differing temperatures through photoperiodic time.

		Predictor trait measures			
Photoperiod	Accessions	Axis 1	Axis 2	Axis 1	Axis 2
Axis 1		Weight		Weight^2	
	Axis 1	**−3.89**[z]	**8.40**	**15.11**	**70.62**
	Axis 2	**8.19**	2.97	**67.14**	8.82
	Axis 3	0.60	1.87	0.36	3.51
Axis 2					
	Axis 1	−3.04	0.18	9.26	0.03
	Axis 2	−2.28	−0.15	5.18	0.02
	Axis 3	**4.50**	1.64	**20.28**	2.70

[z]Bolded combinations contributed greatest to the variation of the dataset.

Table 5. Tucker decomposition loadings by mode for measured traits, photoperiodic times, and applied temperatures resulting from the reduction of higher-order interaction effects of grapevine response to simulated fall conditions between differing temperatures.

		Axis 1	Axis 2
Mode	Level	Axis score	
Measured traits			
	Stem length (cm)	−0.313	−0.144
	Nodes (no.)	−0.350	−0.297
	Mature buds (no.)	0.346	−0.029
	Lateral shoots (no.)	**−0.544**[z]	−0.037
	Tip abscission (0–5 scale)	0.010	**0.901**
	Periderm (cm)	**0.456**	−0.208
	Periderm (no. nodes)	0.394	−0.186
	Portion of total variation (%)	41.61	30.39
Photoperiodic times (daylight h)			
	15.0	**0.384**	**−0.384**
	14.5	0.387	−0.248
	14.0	0.34	−0.045
	13.5	0.284	0.154
	13.0	0.166	0.408
	12.5	−0.045	**0.445**
	12.0	−0.199	0.383
	11.5	−0.291	0.079
	11.0	−0.355	−0.11
	10.5	−0.354	−0.295
	10.0	**−0.318**	**−0.387**
	Portion of total variation (%)	58.71	13.28
Applied temperatures (°C)			
	10	**0.7071**	
	27	**−0.7071**	
	Portion of total variation (%)	100.00	

[z]Bolded values indicate local minimums and maximums for each axis.

with each of the retained genotypic axes, similar relationships were determined as with SVD; however, the photoperiodic timing of events was altered (Table 6). Axis 1 related to relative tip progress through photoperiodic time from 15.0 to 14.5 h of daylight to 11.0 to 10.5 h of daylight across the tested temperatures. Axis 2 contrasted the relative amounts of active growth and tissue maturation early in the season to those later. This axis also associated tip abscission progress as a trait having a similar trend to that of tissue maturation in contrast with the SVD model. Last, Axis 3 was associated with a parabolic distortion of Axis 2 through linear time between the two tested temperatures. The axis was also related to contrasts of late tip abscission progress between 13.0 and 10.0 h of daylight.

Accessions. When the Tucker model was used, three significant axes contributing 33.69%, 28.78%, and 9.52% of the total variation, respectively, were found to describe the 60 accession-by-run combination samples. Two of these axes showed significant variation among accessions following ANOVA (Table 3). The resulting axes had similar relationships to those discovered through SVD. Axis 1 was positively associated with 'Frontenac', 917, and 73 while being negatively associated with 'MN 1131' and its progeny (900, 903, and 906), 909, 914, and 937. The mean of tested riparian grapevines was found to be moderately and positively associated with the axis. The remaining check vine, 'Marquette', was moderately negatively associated with the axis and differed from the mean of tested riparian grapevines.

Axis 2 was associated with 900, 'MN 1131', and riparian grapevines. This axis was negatively associated with four of the five progenies derived from 'ES 8-2-43', 73, and 'Marquette'. The remaining check vine, 'Frontenac', was slightly negative along the axis, but did not differ from the mean of riparian grapevine accessions. Overall, several accessions did not statistically differ from riparian grapevines along both axes having significant variation among accessions. These included accessions derived from 'St. Croix' (911 and 913) and 'ES 8-2-24' (917, 920, and 924) along with 64 as well as 'Frontenac'.

Distinct riparian grapevine and nonriparian grapevine groups were defined when all three retained components were clustered using the Euclidean distance and Ward's minimum variance linkage (Fig. 1). 'Frontenac' and all five wild riparian grapevines clustered together. 'MN 1131' and 'Marquette' each defined subclasses of the nonriparian grapevine group. 'MN 1131' tended to cluster with its progeny, whereas 'Marquette' tended to cluster with members of the 'ES 8-2-43' family.

Comparison of model relationships

When resampling with replacement was used to test the consistency of the predictions, differences were found between the methods in their accuracy in comparison with observed values, as well as in subspace consistency. The sum of squared deviations from observed values was significantly higher and the sum of squared deviations from the full model solution using all samples was lower for Tucker decomposition when compared with SVD (Table 7).

Discussion

Model comparison. Following quadruple centering of the data, all that remained was the effect of the four-way interaction, as all main-effect means, two-way interactions, and three-way interactions were removed (Kroonenberg, 2008). Through the quadruple centering of data, the two investigated temperatures were reduced to reciprocals of one another, as either was equidistant from the mean. This effectively reduced the solutions of each analysis to a three-mode dataset of differences across temperatures.

Table 6. Factor weights of seven predictor variables across photoperiodic time determined using Tucker decomposition of higher-order interaction effects in grapevine response to simulated fall conditions under differing temperatures for the first three retained axes.

		Daylight (h)										
Axis	Trait[z]	15.0	14.5	14.0	13.5	13.0	12.5	12.0	11.5	11.0	10.5	10.0
1												
	L	0.26[y]	0.17	0.03	−0.11	−0.28	−0.31	−0.26	−0.05	0.08	0.21	0.27
	N	0.61	0.51	0.32	0.12	−0.17	−0.37	−0.46	−0.31	−0.22	−0.08	0.02
	MAT	0.15	0.26	0.37	0.46	0.52	0.30	0.07	−0.28	−0.51	−0.65	−0.68
	LAT	−0.05	−0.22	−0.40	−0.57	−0.72	−0.48	−0.20	0.29	0.61	0.84	0.9
	TIP	−2.12	−2.15	−1.90	−1.60	−0.97	0.21	1.08	1.62	2.00	2.01	1.82
	PL	0.60	0.75	0.84	0.91	0.87	0.35	−0.12	−0.68	−1.05	−1.24	−1.24
	PN	0.53	0.66	0.74	0.79	0.76	0.30	−0.11	−0.60	−0.92	−1.09	−1.09
2												
	L	1.25	1.17	0.92	0.64	0.17	−0.40	−0.76	−0.81	−0.85	−0.73	−0.58
	N	1.54	1.45	1.14	0.82	0.24	−0.47	−0.93	−1.01	−1.08	−0.94	−0.76
	MAT	−1.18	−1.10	−0.85	−0.58	−0.12	0.41	0.74	0.75	0.78	0.65	0.50
	LAT	1.94	1.81	1.40	0.96	0.22	−0.66	−1.20	−1.24	−1.29	−1.09	−0.85
	TIP	−0.98	−0.96	−0.82	−0.66	−0.34	0.17	0.53	0.71	0.84	0.81	0.71
	PL	−1.38	−1.27	−0.96	−0.64	−0.09	0.51	0.88	0.86	0.87	0.70	0.53
	PN	−1.19	−1.09	−0.83	−0.55	−0.08	0.44	0.75	0.74	0.74	0.60	0.45
3												
	L	−1.20	−0.61	0.22	1.01	1.97	1.87	1.42	−0.01	−0.90	−1.71	−2.06
	N	−1.31	−0.57	0.44	1.41	2.56	2.33	1.68	−0.16	−1.31	−2.32	−2.75
	MAT	1.37	0.83	0.04	−0.73	−1.69	−1.75	−1.44	−0.20	0.58	1.32	1.67
	LAT	−2.13	−1.24	0.06	1.31	2.87	2.89	2.32	0.22	−1.09	−2.32	−2.88
	TIP	−0.17	−0.73	−1.34	−1.88	−2.38	−1.59	−0.65	0.98	2.02	2.76	2.97
	PL	1.85	1.24	0.31	−0.61	−1.79	−2.02	−1.79	−0.44	0.39	1.22	1.65
	PN	1.60	1.07	0.27	−0.51	−1.53	−1.73	−1.54	−0.39	0.32	1.04	1.40

[z]L = stem length (centimeters); N = number of nodes; MAT = number of mature nodes; LAT = number of lateral shoots; TIP = tip abscission progress visible rating (0–5), where 0 relates to full active growth and 5 relates to loss of meristem; PL = periderm development length (centimeters); and PN = number of nodes enveloped by periderm development.
[y]Increasing green and red hues indicate increasingly positive and negative associations between the axis with the trait measure at the photoperiodic time, respectively.

Both investigated methods, SVD and the Tucker, identified a similar set of three accession axes. Factors related to the relative tip abscission progress rate, progression rate from active growth to maturation of tissue, and a parabolic trend relating growth and tissue maturation through time. The trait identified to explain the largest portion of the variance of the dataset was the differences in relative tip progression through photoperiodic time between temperatures for the tested accessions relative to the average of accessions. This axis had a linear trend through time and distinguished those accessions that had relatively increased rates of tip abscission at 27 °C relative to 10 °C as compared with accessions that had relatively increased rates at 10 °C relative to 27 °C. Native accessions and similar interspecific hybrids tended to have an amplification of tip abscission progress under warmer conditions, whereas dissimilar accessions tended to have similar or decreased rates of tip abscission progress under 27 °C relative to 10 °C.

Table 7. Comparison of decomposition method effect on observed values and full model predictions using 10,000 iterations of resampling with replacement (50 train: 10 test) validation in the reduction of higher-order interaction effects in grapevine responses to simulated fall conditions under differing temperatures across photoperiodic time quantified through multiple predictor traits.

	Observed values			Full model prediction[z]		
	SSD[y]					
Tucker decomposition	13.876	±	0.046	0.11679	±	0.00187
Singular value decomposition	13.687	±	0.045	0.28998	±	0.00324

[z]Predicted values through decompositions using all observed samples.
[y]Average sum of squared deviations ± 95% confidence interval.

The contrast between relative growth and tissue maturation was divided into a linear and a parabolic trend in time as two axes in either model. The linear trend contrasted the rates of change in either trait as they differed across the two temperatures early vs. late in the season and was interpreted as the rate of transition from active growth to tissue maturation. The parabolic trend was explained as a distortion from the linear trend comparing the relative ratio of growth to tissue maturation due to the differing photoperiodic timing of the induction of acclimation responses across the tested accessions. Similar distortions are often a consequence of fitting linear models to nonlinear trends. These may be caused by the shift of a monotonic curve in time. In this instance, the trend was determined to be the consequence of differing initiation points of the morphological transition, or the comparative timing of acclimation initiation as it differed between the two temperatures among cultivars.

The two models differed in the contribution of either's third axis to the variance among accessions, as it was found to be significant using SVD and was not while using the Tucker model, having P values of 0.0432 and 0.0976, respectively. Overall, SVD did account for a greater proportion of the variance among

samples (74.4%) in comparison with the Tucker reduction (72%). The modeling of this additional information may account for the ability to detect significance of Axis 3 of the SVD reduction in comparison with the Tucker solution.

Similar traits were identified in previous study (Stenger and Hatterman-Valenti, 2017). Stenger and Hatterman-Valenti (2017) used Tucker decomposition to identify important acclimation trends of cold-climate grapevines under field conditions in mature vines. Overall, similar axes related to the rate of tip abscission and the transition from active growth to dormant tissue development were identified in related cultivars. This previous work did not identify the parabolic trend related to the timing of acclimation response similar to that reported by Garris et al. (2009). However, the field study did not include accessions from the *V. riparia* × 'Seyval' background. 'Seyval' is a French-American interspecific hybrid grapevine with its majority of parentage derived from common grapevine with lesser portions of American native *Vits rupestris* and *Vitis aestivalis* used to derive disease resistance. In addition, the prior study only accounted for a small set of cultivars, thus may not have included genetics associated with the trait. The current research provides a more encompassing model of temperature adaptive acclimation traits uniting the findings of Stenger and Hatterman-Valenti (2017) and Garris et al. (2009) by identifying all described traits in a single study.

When clusters using all three retained axes for each model were compared, differences existed in the ability of the model to retain logical clusters of the tested riparian grapevines. The Tucker solution clearly grouped all riparian grapevines together, whereas SVD split these accessions among groupings. Based on the goal of identifying riparian grapevine-like accessions, the most concise clustering was created by use of the Tucker model.

Either reduction method led to similar axes; however, the total percent variation and the allocation of error in these axes differed, as all three axes contained significant variation in SVD, whereas the Tucker model resulted in a reduced set of two axes. Similarity among identified axes between bilinear and multiway methods has been reported in the past. Dyrby et al. (2005) concluded that despite such similarities, multiway analysis was still advantageous as results were more interpretable as each mode was decomposed separately. In the current study, the Tucker solution was better in separating wild-type and interspecific hybrid samples compared with bilinear modeling using a combination-mode matrix. In addition, repeated sampling demonstrated that although SVD consistently explained more variance, the subspace it defined was more variable, indicating that the model was overfitting to the data and may be less accurate when predicting performance of new populations. Last, in agreement with previous comparisons, it was determined that because of the ability of the Tucker model to separate trends, results were more easily interpreted and had greater meaning compared with those obtained through SVD of a combination-mode matrix.

Comparison of accessions. The environmental responses of riparian grapevine derived cold-climate hybrids were similar to those found in *Populus* hybrids. Tanino et al. (2010) outlined two methods of temperature-photoperiod related dormancy induction. In *Populus* hybrids, they found that night temperature was correlated with days to growth cessation, rate of growth cessation, depth of dormancy, and both the rate and depth of cold hardiness; whereas only rate of dormancy development was significantly correlated with daytime temperatures. In the current study, the cold-climate adapted riparian grapevines showed a large increase in responsiveness when temperature was increased, particularly in tip abscission and the rate of growth cessation and mature tissue development across the two temperatures when compared with those accessions exhibiting alternate responses. In hybrid progeny of riparian grapevine crossed with nonadapted types, these abilities were separable. All tested industry checks preformed similarly to riparian grapevines in the timing of the transition from active growth to tissue maturation. This is reasonable, as investigations into early initiation of acclimation response have occurred for some time (Fennell and Hoover, 1991; Fennell et al., 2005; Garris et al., 2009; Wake and Fennell, 2000). Adapted types 'Frontenac' and 'MN 1131' displayed additional but separate alternate temperature-based responses in common with riparian grapevines in effect of temperature on the rate of tip abscission and growth cessation and rate of mature tissue development, respectively. In addition, these traits were combinable, as accession 917 had temperature reactive acclimation traits indistinguishable from riparian grapevines and contrasting those of 'Marquette' (Fig. 2). This demonstrates that breeding of cultivars having more similar fall response profiles to wild-type riparian grapevine is possible.

On comparison of clustering based on the data reduction, the california grapevines did not create an outgroup as intended, despite their lack of relationship to the remaining accessions on the species level. It was hypothesized that the species would react differently in comparison with riparian grapevines because of the differing climates of their geographic origins. These results suggest commonality among riparian and california grapevines in acclimation responses, particularly in the rate of tip abscission through time, as well as the timing of transition from active growth to tissue maturation tested between temperatures. Included is the suspected photoperiodic response, which was identified as a parabolic distortion in time, and was tied to differences in genotypic trends in lateral shoot development (Fennell and Hoover, 1991; Fennell et al., 2005; Garris et al., 2009; Wake and Fennell, 2000). Previous research has shown california grapevines to be genetically distinct from the North American and Eurasian species of grapevine (Pèros et al., 2011; Trǒndle et al., 2010; Wan et al., 2013; Zecca et al., 2012). This study demonstrates a similar early occurrence of feed-forward response to photoperiod in the Mediterranean california grapevine species, as was found in the continental species riparian grapevine. California grapevines tended to be distinct from riparian grapevine along the axis relating to rate of transition from active growth to tissue maturation, as their axes differed for both tested models. This adaptation may afford california grapevines the ability to take advantage of extended cool seasons, as growth and tissue maturation were not hindered; whereas riparian grapevines had increased benefit in growth cessation and tissue maturation when temperatures were increased to force early acclimation in a relatively unstable native continental climate.

Overall, beyond the early photoperiod-based induction that was previously described, the rate of transition from active growth to tissue maturation was a discernable trait of riparian grapevine. In addition, the trait contributing greatest to the variation in the dataset was the differences in tip abscission progress rate between the two temperatures over photoperiodic time. Those grapevines similar in response to riparian grapevines tended to be temperature sensitive in their responses, having greater increases in reaction across the two temperatures when

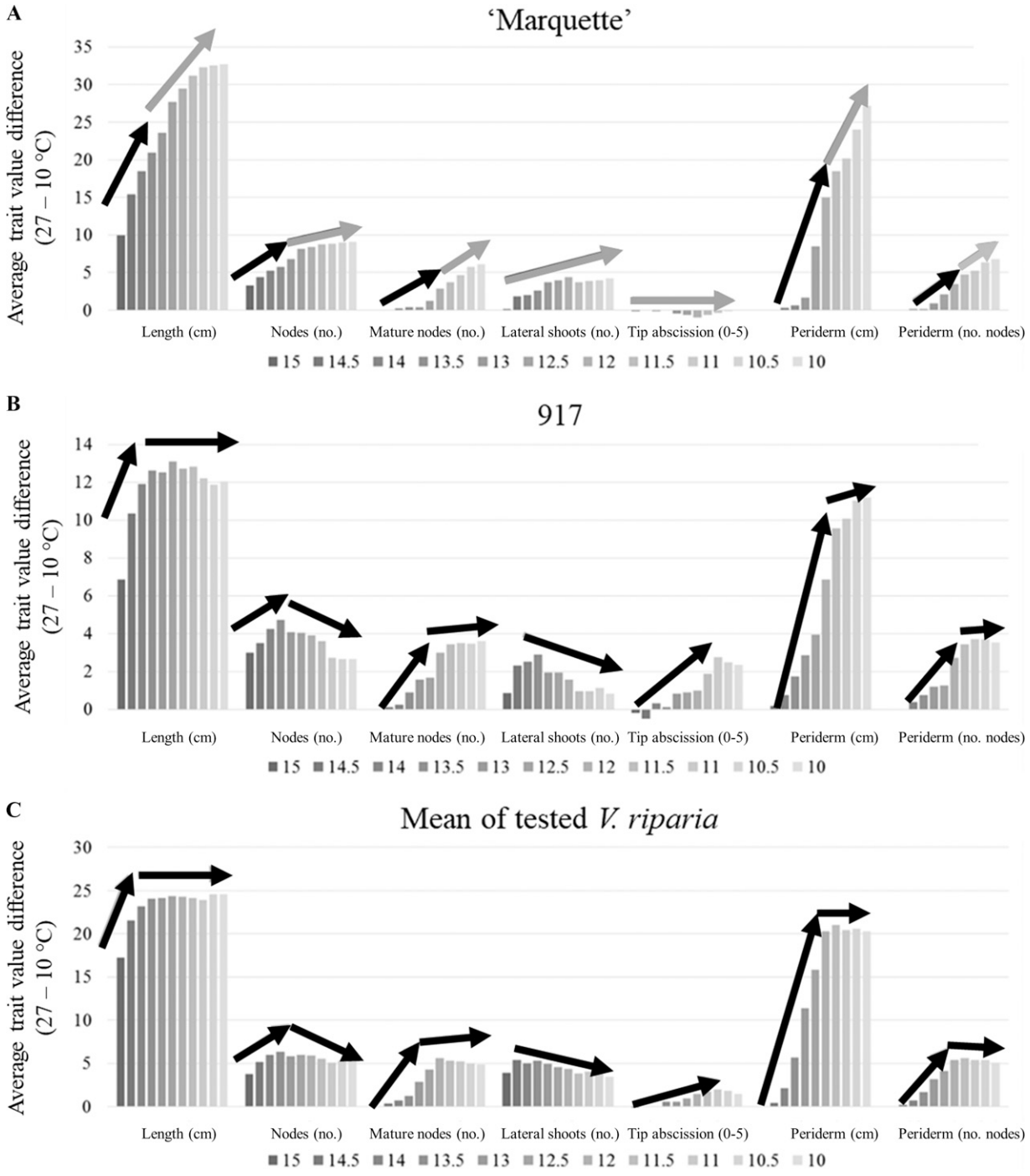

Fig. 2. Comparison of the trends of response differences to simulated fall conditions of selected grapevines (**A**) 'Marquette', (**B**) 917, and (**C**) the mean of riparian grapevines between temperatures for seven predictor variables across photoperiodic time (15 to 10 h of daylight). Tip abscission progress visible rating was on a 0 to 5 scale, where 0 relates to full active growth and 5 relates to loss of meristem. Black and gray arrows indicate trends consistent with and those opposed to identified responses of riparian grapevines, respectively.

compared with an average vine. 'MN 1131' was found to be an adaptive type that combined early acclimation response with temperature adaptive progression in its transition from active growth to tissue maturation. 'Frontenac' displayed an alternative adapted method, as it had early induction of acclimation response coupled with temperature adaptive tip abscission rate across the tested temperatures. 'Marquette' did not differ from riparian grapevines in acclimation initiation timing where the trait was found to statistically differ across accessions; however, it did differ for the additional adaptive responses involving the influence of temperature on the rate of progress of both tip abscission and the transition from active growth to tissue maturation.

The conclusions of this study indicate, in part, that the inclusion of either rate adaptive response of tip progression or transition from active growth to tissue maturation, along with early acclimation initiation may enable productive cultivars in the

northern Plains region of the United States. However, the exclusion of both rate adaptive responses, even with early initiation, may leave cultivars unreliable in the region. 'Frontenac' and 'MN 1131' had additional temperature reactive traits over that of 'Marquette', aligning with pre-experiment perceptions of the regional adaptation of the cultivars (Hatterman-Valenti et al., 2016). In addition, the accession 917 was found to be indistinguishable from riparian grapevines demonstrating the potential for wild-type adaptation feature reconstruction in interspecific hybrid backgrounds.

Conclusions

The overall similarity of the identified axes, increased ability to differentiate riparian grapevines from other accessions, defining of a more stable subspace, and simplification of the interpretation of the identified axes suggests that the Tucker model will be more practical for investigating high-order trait response profiles as compared with bilinear models. The characterization of multiway trends through the decomposition of higher-order reactions was an efficient and relatively high-throughput method for characterizing samples in a controlled repeatable experiment and has plant breeding implications. The method identified traits characterized in previous studies in a single more encompassing model. The reduction of higher-order interaction was found to be useful in gaining insight into the relative effects of multiple environmental cues on a particularly difficult to characterize trait in photoperiod-based acclimation response. The use of the methodology described here is likely to have further utility in the characterization of many complex traits in other crops and biological systems. Overall, the inclusion of such methodologies for crop improvement for a wide array of difficult-to-quantify adaptation, resistance, quality, and developmental processes may have benefit in *Vitis* as well as in other woody, perennial, or annual crops. Such methods may aid in preserving diversity in quantitative traits as compromises in trait similarities are made. Overall, the evaluation of process traits may aid to improve breeding for the future, especially when applied to the adaptation of germplasm to nontraditional growing regions. Such methods can have further utility in other areas of plant science, from aiding in the characterization of plant genetic expression and physiology to landscape-level ecological systems as a multiway extension of reaction norms.

Literature Cited

Andersson, C.A. and B. Bro. 2000. The N-way Toolbox for MATLAB. Chemom. Intell. Lab. Syst. 52:1–4, https://doi.org/10.1016/S0169-7439(00)00071-X.

Burke, M.J., L.V. Gusta, H.A. Quamme, C.J. Weiser, and P.H. Li. 1976. Freezing and injury in plants. Ann. Rev. Plant Physiol. 27: 507–528, https://doi.org/10.1146/annurev.pp.27.060176.002451.

Chapman, S.C., J. Crossa, K.E. Basford, and P.M. Kroonenberg. 1997. Genotype by environment effects and selection for drought tolerance in tropical maize II Three-mode pattern analysis. Euphytica 95: 11–20, https://doi.org/10.1023/A:1002922527795.

Cong, F., Q. Lin, L. Kuang, X. Gong, P. Astikainen, and T. Ristaniemi. 2015. Tensor decomposition of EEG signals: A brief review. J. Neurosci. Methods 248:59–69, https://doi.org/10.1016/j.jneumeth.2015.03.018.

Dyrby, M., D. Baunsgaard, R. Bro, and S.B. Engelsen. 2005. Multiway chemometric analysis of the metabolic response to toxins monitored by NMR. Chemom. Intell. Lab. Syst. 76:79–89, https://doi.org/10.1016/j.chemolab.2004.09.008.

Fennell, A. and E. Hoover. 1991. Photoperiod influences growth, bud dormancy, and cold acclimation in *Vitis labruscana* and *V. riparia.* J. Amer. Soc. Hort. Sci. 116:270–273, https://doi.org/10.21273/JASHS.116.2.270.

Fennell, A., K. Mathiason, and J. Luby. 2005. Genetic segregation for indicators of photoperiod control of dormancy induction in *Vitis* species. Acta Hort. 689:533–539, https://doi.org/10.17660/ActaHortic.2005.689.66.

Fennell, A., K.A. Schlauch, S. Gouthu, L.G. Deluc, V. Khadka, L. Sreekantan, J. Grimplet, G.R. Cramer, and K.L. Mathiason. 2015. Short day transcriptomic programming during induction of dormancy in grapevine. Frontiers Plant Sci. 6:834, https://doi.org/10.3389/fpls.2015.00834.

Flores, F., M.T. Moreno, and J.I. Cubero. 1998. A comparison of univariate and multivariate methods to analyze G × E interaction. Field Crops Res. 56:271–286, https://doi.org/10.1016/S0378-4290(97)00095-6.

Garris, A., L. Clark, C. Owens, S. McKay, J. Luby, K. Mathiason, and A. Fennell. 2009. Mapping of photoperiod induced growth cessation in the wild grape *Vitis riparia*. J. Amer. Soc. Hort. Sci. 134:261–272, https://doi.org/10.21273/JASHS.134.2.261.

Goodacre, R., D. Broadhurst, A.K. Smilde, B.S. Kristal, J.D. Baker, R. Beger, C. Bessant, S. Connor, G. Capuani, A. Craig, T. Ebbels, D.B. Kell, C. Manetti, J. Newton, G. Paternosto, R. Somorjai, M. Sjöström, J. Trygg, and F. Wulfert. 2007. Proposed minimum reporting standards for data analysis in metabolomics. Metabolomics. 3:231–241, https://doi.org/10.1007/s11306-007-0082-2.

Hatterman-Valenti, H.M., C.P. Auwarter, and J.E. Stenger. 2016. Evaluation of cold-hardy grape cultivars for North Dakota and the North Dakota State University germplasm enhancement project. Acta Hort. 1115:13–22, https://doi.org/10.17660/ActaHortic.2016.1115.3.

Hemstad, P. 2015. Grapevine breeding in the Midwest, p. 411–426. In: A. Reynolds (ed.). Grapevine breeding programs for the wine industry. Woodhead Publ., Waltham, MA.

Hemstad, P.R. and J.J. Luby. 2000. Utilization of *V. riparia* for the development of new wine varieties with resistance to disease and extreme cold. Acta Hort. 528:487–496, https://doi.org/10.17660/ActaHortic.2000.528.70.

Kroonenberg, P.M. (ed.). 2008. Applied multiway data analysis. Wiley, Hoboken, NJ.

Légère, A. and N. Samson. 1999. Relative influence of crop rotation, tillage, and weed management on weed associations in spring barley cropping systems. Weed Sci. 47:112–122, https://www.jstor.org/stable/4046244.

Luciano, G. and T. Næs. 2009. Interpreting sensory data by combining principal component analysis and analysis of variance. Food Qual. Prefer. 20:167–175, https://doi.org/10.1016/j.foodqual.2008.08.003.

Mørup, M. 2011. Applications of tensor (multiway array) factorizations and decompositions in data mining WIREs. Data Min. Knowl. Discov. 1:24–40, https://doi.org/10.1002/widm.1.

Nesaragi, N., S. Patidar, and V. Aggarwal. 2021. Tensor learning of pointwise mutual information for HER data for early prediction of sepsis. Comput. Biol. Med. 134:104430, https://doi.org/10.1016/j.compbiomed.2021.104430.

Nomme, K.M. and P.G. Harrison. 1991. A multivariate comparison of the seagrasses *Zostera narina* and *Zostera japonica* in monospecific mixed populations. Can. J. Bot. 69:1984–1990, https://doi.org/10.1139/b91-249.

Pèros, J., G. Berger, A. Portemont, J. Boursiquot, and T. Lacombe. 2011. Genetic variation and biogeography of the disjunct *Vitis* subg. *Vitis* (Vitaceae). J. Biogeogr. 38:471–486, https://doi.org/10.1111/j.1365-2699.2010.02410.x.

Piepho, H. 1999. Stability analysis using the SAS system. Agron. J. 91:154–160, https://doi.org/10.2134/agronj1999.00021962009100010024x.

Schnabel, B.J. and R.L. Wample. 1987. Dormancy and cold hardiness in *Vitis vinifera* L. cv. White Riesling as influenced by photoperiod and temperature. Amer. J. Enol. Viticult. 38:265–272.

Smita, S., M. Robben, A. Deuja, M. Accerbi, P.J. Green, S. Subramanian, and A. Fennell. 2021. Integrative analysis of gene expression and miRNAs reveal biological pathways associated with bud paradormancy and endodormancy in grapevine. Plants (Basel) 10:669, https://doi.org/10.3390/plants10040669.

Stenger, J.E. and H. Hatterman-Valenti. 2017. Contrasting responses to environmental conditions by three cold-climate winegrape cultivars grown in the United States Northern Plains region. Acta Hort. 1188:173–180, https://doi.org/10.17660/ActaHortic.2017.1188.23.

Swenson, E. 1982. 'SD 62-8-160' Grapevine. U.S. Patent Plant 4,928. Filed 11 Feb. 1981. Issued 9 Nov. 1982.

Tanino, K.K., L. Kalcsits, S. Silim, E. Kendall, and G.R. Gray. 2010. Temperature-driven plasticity in growth cessation and dormancy development in deciduous woody plants; a working hypothesis suggesting how molecular and cellular function is affected by temperature during dormancy induction. Plant Mol. Biol. 73:49–65, https://doi.org/10.1007/s11103-010-9610-y.

Teh, S.K., W. Zheng, K.Y. Ho, M. Teh, K.G. Yeoh, and Z. Huang. 2010. Near-infrared Raman spectroscopy for early diagnosis and typing of adenocarcinoma in the stomach. Br. J. Surg. 97:550–557, https://doi.org/10.1002/bjs.6913.

Tomic, N., D. Rodivojevic, J. Milivojevic, I. Djekic, and N. Smigic. 2016. Effects pf 1- methylcyclopropene and diphenylamine on changes in sensory properties of 'Granny Smith' apples during postharvest storage. Postharvest Biol. Technol. 112:233–240, https://doi.org/10.1016/j.postharvbio.2015.09.009.

Tröndle, D., S. Schröder, H. Kassemeyer, C. Kiefer, M.A. Kock, and P. Nick. 2010. Molecular phylogeny of the genus *Vitis* (Vitaceae) based on plastid markers. Amer. J. Bot. 97:1168–1178, https://doi.org/10.3732/ajb.0900218.

Wake, C.M.F. and A. Fennell. 2000. Morphological, physiological and dormancy responses of three Vitis genotypes to short photoperiod. Physiol. Plant. 109:203–210, https://doi.org/10.1034/j.1399-3054.2000.100213.x.

Wan, Y., H.R. Schwaninger, A.M. Baldo, J.A. Labate, and G. Zhong. 2013. A phylogenetic analysis of the grape genus (*Vitis* L.) reveals broad reticulation and concurrent diversification during Neogene and quaternary climate change. BMC Evol. Biol. 13:141, https://doi.org/10.1186/1471-2148-13-141.

U.S. Department of Agriculture, Agricultural Research Service. 2022. GRIN-Global. U.S. National Plant Germplasm System. 14 Feb. 2022. <https://npgsweb.ars-grin.gov/gringlobal/search>.

Van Eeuwijk, F.A. and P.M. Kroonenberg. 1998. Multiplicative models for interaction in three-way ANOVA, with applications to plant breeding. Biometrics 54:1315–1333, https://doi.org/10.2307/2533660.

Zecca, G., J.R. Abbott, W. Sun, A. Spada, F. Sala, and F. Grassi. 2012. The timing and the mode of evolution of wild grapes (*Vitis*). Mol. Phylogenet. Evol. 62:732–747, https://doi.org/10.1016/j.ympev.2011.11.015.